



A novel selective "turn-on" fluorescent sensor for Hg²⁺ and its utility for spectrofluorimetric analysis of real samples

Süreyya Oğuz TÜMAY*  

Department of Chemistry, Gebze Technical University, Gebze 41400, Kocaeli, Turkey.

Abstract: A novel anthracene-based dipodal Schiff base "turn-on" fluorescent sensor (**FS**) was designed and synthesized by accessible and straightforward Schiff base reaction of salicylaldehyde and 9,10-bis(aminomethyl)anthracene with high yield. The chemical characterization of fluorescent sensor **FS** was performed by standard spectroscopic techniques (MALDI-MS, FT-IR, ¹H, and ¹³C NMR), and photophysical properties were examined by UV-vis and fluorescent spectroscopies. The fluorescent sensor **FS** can coordinate with Hg²⁺ via Schiff base moiety when analytical signal as a "turn on" fluorescent response was obtained via anthracene moiety after coordination. Also, spectrofluorimetric analysis of Hg²⁺ was carried out using fluorescent sensor **FS** in environmental water samples after optimization required experimental conditions such as pH, the time before measurements, and photostability. According to obtained results, the presented fluorescent sensor can be used for selective and sensitive spectrofluorimetric determination of Hg²⁺.

Keywords: Schiff base, Fluorescent sensor, Spectrofluorimetry, Water samples, Mercury(II).

Submitted: May 06, 2020. **Accepted:** May 15, 2020.

Cite this: TÜMAY SO. A novel selective "turn-on" fluorescent sensor for Hg²⁺ and its utility for spectrofluorimetric analysis of real samples. JOTCSA. 2020;7(2):505-16.

DOI: <https://doi.org/10.18596/jotcsa.733160>.

***Corresponding author. E-mail:** sotumay@gtu.edu.tr. Tel: 00 90 262 6053106, Fax: 00 90 262 6053105.

INTRODUCTION

Although industrial and technological activities increase the quality of our life, it causes severe problems for environmental pollution and human health. Contamination of the environment with heavy metal ions led to potential damage to mankind due to the highly toxic effect of these ions even at low concentrations (1). Between these metal ions, Hg²⁺ is one of the most hazardous heavy metal ions because it can inhibit the activity of some biological species such as enzymes and proteins (2). Besides, it can be accumulating to the human body via the food chain and causes severe diseases of the central nervous system (3-5). Therefore, the United States Environmental Protection Agency (EPA) and World Health Organization (WHO) strongly limited the permissible concentration of Hg²⁺ ions in drinking

water in the range of several ppb (µg/kg) (6, 7). Although a significant number of analytical methods are used for detection and determination of Hg²⁺ ions up to now such as capillary electrophoresis (CE), liquid chromatography (LC), atomic absorption spectrometry (AAS), gas chromatography (GC), and atomic fluorescent spectrometry (AFS), these methods generally require preconcentration processes with extra chemicals (adsorbents or eluents), applied by expert users. In addition, they are not applied to in-field analysis (8-11). Fluorescent sensors, handling these disadvantages, attract attention for detection and determination of Hg²⁺ ions due to their several advantages such as simple operation, high sensitivity and selectivity, low cost, and real-time monitoring in-field analysis (12-14). Notably, the development of "turn-on" fluorescent sensors, which are selective for Hg²⁺, has become an

important research topic due to their increased sensitivity compared to “turn-off” fluorescent sensors. Because they can detect analytes via fluorescent signal increment, which led to more easy monitoring than fluorescent sensors that can detect analytes with fluorescent quenching (15-17), another important phenomenon is that heavy metal ions such as Hg^{2+} are known as quencher due to spin-orbit coupling (18). Therefore, developing a selective, sensitive, new, and simple “turn-on” fluorescent sensor for Hg^{2+} ions, which can be practicable to the spectrofluorimetric analysis of the environmental and biological sample is still an essential research area (19, 20).

Schiff bases, which are the essential class of organic compounds, can be obtained with the moderate reaction of primary amines with aldehydes/ketones. These kinds of compounds generally offer one-step synthesis processes in moderate conditions with high yield. Also, an imine bond, known as carbon-nitrogen double bond ($-\text{C}=\text{N}-$), is obtained as a result of Schiff base reaction can readily be used for coordination with metals (7, 21, 22). After coordination with metal ions, inhibition of the $\text{C}=\text{N}$ isomerization cause substantial fluorescent enhancement for such molecules, which is used as obtaining analytical signals (23). Also, according to previously published reports, it is well-known that via sulfur, oxygen, or nitrogen atoms, mercury ions can coordinate with fluorescent sensors (7, 13, 24). Therefore, Schiff base preparation methods can be used for obtaining Hg^{2+} ion-selective fluorescent sensors that containing anthracene with proper cavity and donor atoms due to its well-known optical and metal-binding properties (7, 25, 26). There are a few papers that existed in the literature regarding the develop fluorescent sensors, which are used for selective and sensitive detection of Hg^{2+} based on anthracene containing Schiff base systems (23, 27). However, some deficiencies regarding selectivity and applicability were observed in these reports (27). Thus, in this study, simple, accessible, and non-sulfur anthracene-based dipodal Schiff base fluorescent sensor for selective, sensitive, and simple quantification of Hg^{2+} ion in environmental water samples was prepared by the reaction of salicylaldehyde and 9,10-bis(aminomethyl)anthracene with high yield. The nitrogen and oxygen donor atoms provide the coordination capacity for Hg^{2+} ions (7, 13, 24) when anthracene core acts as a fluorophore for obtaining analytical signals. After full characterization of novel fluorescent sensor by MALDI-MS, FT-IR, NMR spectroscopies, required conditions were optimized and spectrofluorimetric determination of Hg^{2+} ions were carried out in environmental water samples.

EXPERIMENTAL

Materials and Instrumentation

The reagents and solvents which are used for preparation and fluorescent sensor application of **FS** purchased from commercially as follows: Anthracene, dichloromethane, 2-bromoethanol, paraformaldehyde, cetyltrimethylammonium bromide (CTAB), glacial acetic acid from Merck, 2,5-dihydroxybenzoic acid (MALDI-MS matrix) from Fluka, deuterated DMSO from Sigma-Aldrich and they were used as received. Inert argon atmosphere was used for the synthesis of **FS**.

Varian Eclipse spectrofluorometer and Shimadzu 2101 UV spectrophotometer were used for recording fluorescent and the electronic absorption spectra of **FS** in the UV-vis region. Also, spectrofluorimetric analysis in environmental water samples where 5 nm of slit width and 1 cm of path-length were used for all fluorescent measurements at 25°C were performed by Varian Eclipse spectrofluorometer. NMR (^1H and ^{13}C NMR), FT-IR, and mass analysis of **FS** were recorded with Varian INOVA 500 MHz spectrometer, Perkin Elmer Spectrum 100 spectrophotometer, and Bruker Daltonics Microflex MALDI-TOF mass spectrometer, respectively. Deuterated DMSO was used for all NMR measurements. The non-linear regression calculations were performed using Sigma-Plot 14.0.

All water samples were collected from Kocaeli/Sakarya in Turkey and filtered with filter paper (blue band). After that, they were acidified with nitric acid and kept at 4°C in a refrigerator before the spectrofluorimetric analysis. The presented spectrofluorimetric analysis performed without any enhancement processes via sensitive and selective complexation of **FS** with Hg^{2+} ion. The fluorescent signal of **FS** that raised via anthracene proportionally and gradually increased after treatment with 0.05-120.00 μM of Hg^{2+} . Spectrofluorimetric determination of Hg^{2+} ion in real samples was performed via analytical signals that were obtained by complexation of Hg^{2+} -**FS**, and the calibration curve was used for analysis with relative fluorescent response change. For determination of Hg^{2+} , 6.25×10^{-5} M of **FS** was prepared in DMSO. After taking 0.80 mL of **FS** from this solution, 1.70 mL of DMSO, 0.25 mL of Britton–Robinson buffer solution (pH 8.0), and 0.25 mL of sample was added onto volumetric flask (5 mL). After that, the volume of the flask was completed with deionized water to 5 mL and carefully shaken for 60 seconds. All spectrofluorimetric measurements were recorded at 426 nm.

Synthesis

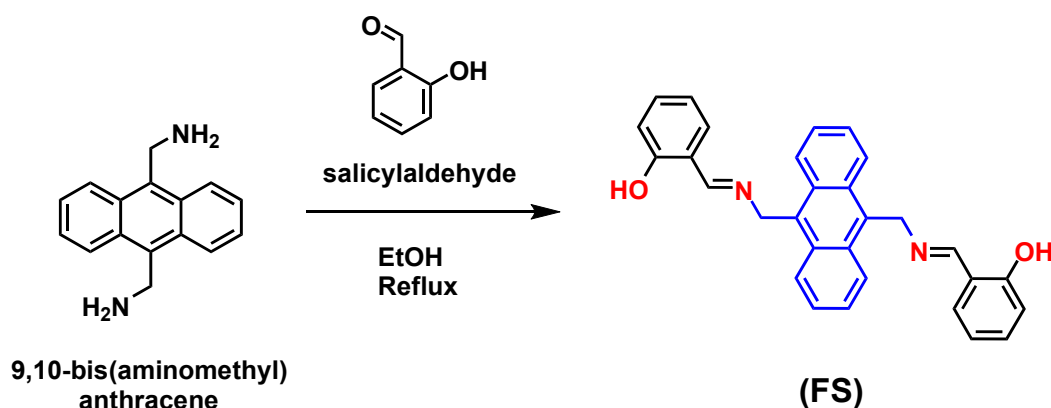
9,10-bis(aminomethyl)anthracene was synthesized and characterized according to literature (28) and **FS** was obtained as follows: 2.460 g of salicylaldehyde (0.0201 mol) dissolved in absolute ethanol in the stream of argon gas and refluxed for 30 minutes. Then, 4.750 g of 9,10-bis(aminomethyl)anthracene (0.0201 mol) and several drops of glacial acetic acid were added onto the solution of salicylaldehyde. The reaction mixture was refluxed during a day. Then the yellow precipitate was filtered with blue filter paper and washed three times with ethanol and n-hexane. **FS** was obtained as a yellow solid with 95% yield (8.488 g). FT-IR; 3271 cm^{-1} (-OH), 3061-3050 cm^{-1} (-ArH), 2917-2867 cm^{-1} (-C-H), 1634 cm^{-1} (-CH=N), 1600-1400 cm^{-1} (-C=C-), 1444.1-1335.1 cm^{-1} (-C-H-). $[\text{M}]^+$: 444.654 m/z (calc. $[\text{M}]^+$: 444.530). ^1H NMR in DMSO- d_6 at 25°C, δ_{ppm} ; 13.38 (s, 2H), 8.90 (s, 2H), 8.58 (dd, $J = 6.7, 3.2$ Hz, 4H), 7.67 (dd, $J = 6.7, 3.2$ Hz, 4H), 7.42 (d, $J = 7.8$ Hz, 2H), 7.27 (t, $J = 7.9$ Hz, 2H), 6.85 (t, $J = 7.5$ Hz, 2H), 6.77 (d, $J = 8.2$ Hz, 2H), 5.88 (s, 4H). ^{13}C NMR in in DMSO- d_6 at 25°C, δ_{ppm} ; 166.10,

160.27, 132.41, 131.72, 130.37, 129.82, 126.31, 125.05, 118.65, 116.41, 53.65.

RESULT AND DISCUSSION

Structural Characterization

The fluorescent sensor (**FS**) having a di-functional primer amine derivative of anthracene core was prepared by following the literature procedure (28). Briefly, 9,10-bis(bromomethyl)anthracene was obtained with high yield (96%) by the reaction of anthracene and HBr in the presence of paraformaldehyde and CTAB. After that, 9,10-bis(aminomethyl)anthracene, which is the di-functional primer amine derivative of anthracene core, was prepared in high yield (95%) by reaction of 9,10-bis(bromomethyl)anthracene and hexamethylenetetramine. Finally, the presented fluorescent sensor (**FS**) was prepared with high yield (95%) as a result of the Schiff base reaction of 9,10-bis(aminomethyl)anthracene and salicylaldehyde in ethanol (Scheme 1). During the preparation of **FS** with high yield, any purification process was not used except for washing and precipitation.



Scheme 1: The synthetic route of **FS**.

The chemical structure of the novel fluorescent sensor was investigated by FT-IR, MALDI-MS, and NMR (^1H and ^{13}C) spectroscopies. All results point out that the proposed structure of **FS** was consistent with characterization data. For instance, The FT-IR spectra of 9,10-bis(aminomethyl)anthracene, salicylaldehyde, and **FS** were depicted in Figure 1a. 9,10-bis(aminomethyl)anthracene demonstrated peaks at 1550 cm^{-1} , 2956-2867 cm^{-1} , 3078-3045 cm^{-1} and 3256-3167 cm^{-1} which assigned to stretching vibrations of -C=C-, -C-H, -ArH and -NH $_2$, respectively. Besides, -C=C-, -OH and -C=O stretching of the aldehyde functional groups of salicylaldehyde were observed at 1555 cm^{-1} , 3142 cm^{-1} and 1662 cm^{-1} , respectively. As can be seen from FT-IR spectra of **FS**, stretching vibrations of -C=C-, -CH=N, -C-H, -ArH and -OH were observed

at 1575 cm^{-1} , 1634 cm^{-1} , 2917-2867 cm^{-1} , 3061-3050 cm^{-1} and 3271 cm^{-1} , respectively (13, 29). Importantly, -C=O stretching of salicylaldehyde (1662 cm^{-1}) and -NH $_2$ stretching of 9,10-bis(aminomethyl)anthracene (3256-3167 cm^{-1}) were disappeared after the formation of **FS** which were important evidence for the proposed structure of **FS**. The ^1H NMR spectrum of **FS**, which recorded in DMSO- d_6 , was demonstrated in Figure 1b. The peak observed at 5.88 ppm was attributed to aliphatic methylene protons, which exist in the anthracene core, and aromatic protons of **FS** were observed between 8.59-6.76 ppm. Also, the imino proton was observed at 8.90 ppm while -OH proton existed at 13.38 ppm as a singlet peak. The integration value ratio of aromatic protons to methylene protons was 4: 1, which is an evidence

of compatibility with the proposed chemical structure.

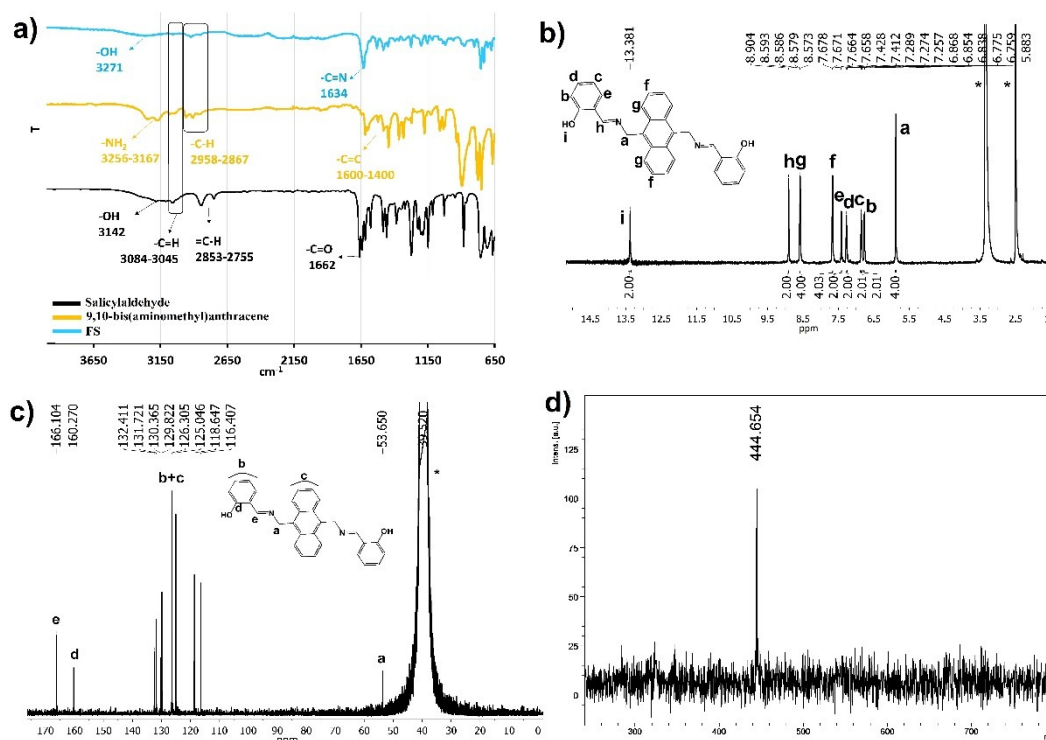


Figure 1: a) FT-IR spectra of 9,10-bis(aminomethyl)anthracene, salicylaldehyde, and **FS**, b) ¹H NMR (in DMSO-d₆), c) ¹³C NMR (in DMSO-d₆) and d) MALDI-MS spectrum of **FS**.

Photophysical Investigation

The photophysical properties of **FS** were investigated using electronic absorption in the UV-Vis region and fluorescent experiments. The effect of various solvents on UV-Vis absorption of 10 μM **FS** was investigated with various solvents such as n-hexane, THF, dichloromethane (DCM), acetonitrile (ACN), ethanol, DMSO, DMF, and water (Figure 2a). The UV-vis electronic absorption of **FS** reached maxima at 258 and 378 nm, which can be assigned to n-n* transition of anthracene moieties (30). Also, UV-Vis electronic absorption properties of **FS** were not changed by solvents except for absorbance values, which are presumably dissolution differences in various solvents. The

fluorescent sensor presented has high solubility in THF, dichloromethane, acetonitrile, DMSO, DMF, while it has low solubility in n-hexane, ethanol, and water only. UV-Vis electronic absorption properties of **FS** were examined at different concentrations in DMSO (Figure 2b). According to Figure 2b, absorbance values were proportionally decreased with decreasing concentrations of **FS** in UV-Vis electronic absorption spectra. The same situation was observed with other tested solvents, and molar absorptivities (ε) of compounds in various solvents were calculated. The fluorescent quantum yield (Φ) and other photophysical properties were summarized at Table 1.

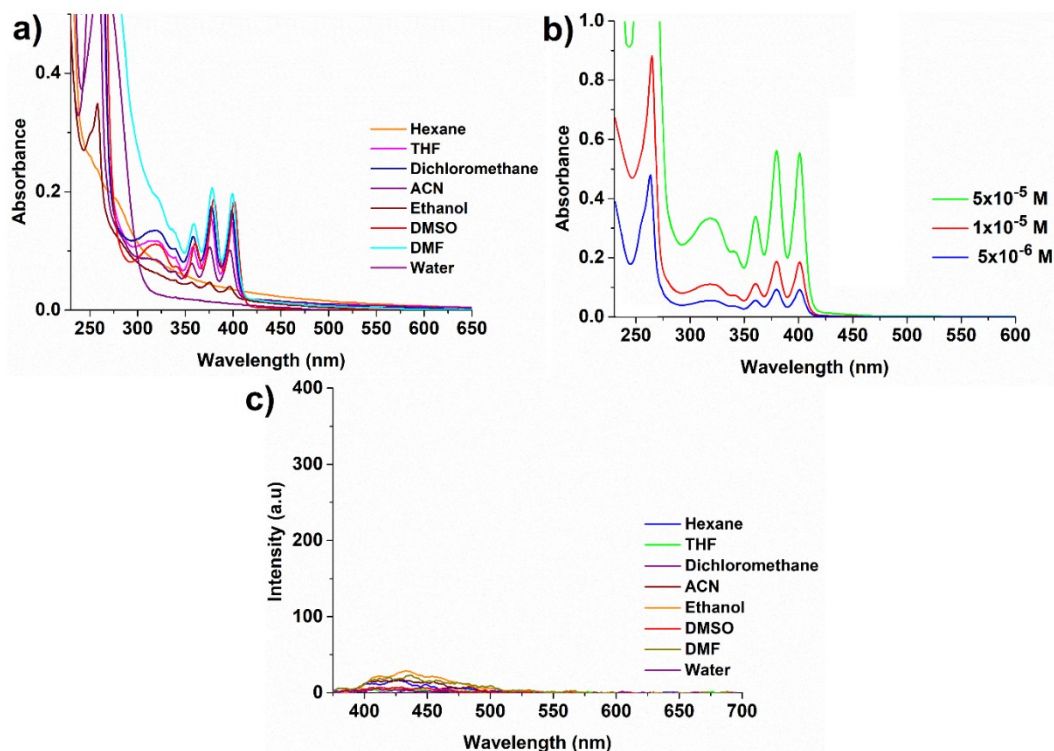


Figure 2: a) UV-Vis electronic absorption of 10 μM **FS** in different solvents, b) UV-vis electronic absorption of different concentrations of **FS** in DMSO, and c) fluorescent emission spectra of 10 μM **FS** in different solvents.

After the evaluation of the electronic absorption properties of **FS**, fluorescent emission properties of **FS** were examined with steady-state fluorescent measurements under the same conditions with UV-Vis absorption studies (Figure 2b). All fluorescent emission spectra of **FS** were recorded at 10 μM when excited at 360 nm. The effect of various solvents on fluorescent emission of **FS** was

investigated with the same solvent systems. In Figure 2b, the fluorescent sensor **FS** showed a very weak fluorescent signal at ~ 420 nm when excited at 360 nm. It is a well-known phenomenon for Schiff base due to photoinduced electron transfer (PET) process from Schiff base to fluorophore group of sensor (7, 23, 27, 29).

Table 1: Photophysical properties of **FS**.

λ_{abs} (nm)	λ_{ems} (nm)		ϵ ($\text{L}\cdot\text{mol}^{-1}\cdot\text{cm}^{-1}$) $\times 10^3$					Φ_f (%)	
			THF	DCM	ACN	Ethanol	DMSO		
FS 258, 378	426 (very weak)	(very	15.1	17.4	9.4	4.3	17.7	19.7	1.44

The fluorescent quantum yield (Φ_f) of **FS** was determined with the comparative method (Eq. (1)) (31). The quinine sulfate was used as a standard

for the calculation of Φ_f , because Φ_f of quinine sulfate was calculated as 0.54 in the literature (in 0.1 M H_2SO_4) (32).

$$\Phi_f = \Phi_{f_{\text{std}}} \frac{F \cdot A_{\text{std}} \cdot n^2}{F_{\text{std}} \cdot A \cdot n_{\text{std}}^2} \quad \text{Eq. (1)}$$

In Eq. (1), F_{std} , A_{std} , F and A represent the areas of fluorescent emission and electronic absorption curves of standard and **FS**, respectively at the excitation wavelengths. Besides, n_{std} and n demonstrate the refractive indices of solvents used for the standard and **FS**, respectively.

Fluorescent Sensor Property of **FS** and Optimization Studies

Fluorescent sensor property and selectivity of 10 μM **FS** was investigated in DMSO:water (pH 8.0, 1:1 v/v) against 120 μM of various metal ions (as nitrate salts) such as Mn^{2+} , Al^{3+} , Cs^+ , Ba^{2+} , Fe^{3+} , Ca^{2+} , K^+ , Cu^{2+} , Pb^{2+} , Hg^{2+} , Zn^{2+} , Mg^{2+} , Na^+ , Li^+ ,

Ni^{2+} , Ag^+ , Fe^{2+} , Cd^{2+} , Co^{2+} , Cr^{3+} by UV-Vis and fluorescent spectroscopies. The UV-Vis electronic absorption spectrum of **FS** significantly changes upon the addition of $120 \mu\text{M}$ Hg^{2+} ion when other metal ions did not cause any change under identical analytical conditions (Figure 3a). The absorption of **FS**, which at long wavelength centered at 378 nm , decreased ($\sim 50\%$) and other absorption, which centered at 258 nm red-shifted as 16 nm and observed at 274 nm . As a result of the electronic reorganization, an important color change was observed from yellow to colorless at daylight (Figure 3b). These changes in the UV-Vis absorption spectrum occurring by the addition of Hg^{2+} to **FS** can be assigned to the electronic reorganization after coordination of **FS** with Hg^{2+} (25, 33).

After the evaluation of UV-Vis response of **FS** towards various metal ions, fluorescent sensor properties of **FS** were investigated using fluorescent spectroscopy under identical analytical conditions with UV-Vis experiments (see Figure 3c); **FS** has a minimal fluorescent signal due to PET process from Schiff base to anthracene moiety when excited at 360 nm (34). After selective complexation of **FS** with the Hg^{2+} cation, the

fluorescent emission of **FS**, which originated from blue monomer emission of anthracene moiety, importantly increased at 426 nm . The change for fluorescent emission can be attributed to the chelation-enhanced fluorescence (CHEF) process, which occurred with selective complexation of **FS** with Hg^{2+} cation, and it inhibited the PET process (34). Importantly, except for Hg^{2+} , other tested metal ions did not demonstrate this effect and cause any "turn on" response on the fluorescent signal of **FS** (Figure 3c). As significant property of fluorescent sensors, selectivity of $10 \mu\text{M}$ **FS** in DMSO:water (pH 8.0, 1:1 v/v) over other competitive metal cations and anions was investigated with addition of Mn^{2+} , Al^{3+} , Cs^+ , Ba^{2+} , Fe^{3+} , Ca^{2+} , K^+ , Cu^{2+} , Pb^{2+} , Hg^{2+} , Zn^{2+} , Mg^{2+} , Na^+ , Li^+ , Ni^{2+} , Ag^+ , Fe^{2+} , Cd^{2+} , Co^{2+} , Cr^{3+} , Cl^- , F^- , NO_3^- , I^- , CO_3^{2-} , SO_4^{2-} . The selectivity studies were performed where concentration of other competitive species was $2400 \mu\text{M}$ (Figure 4). As seen in this figure, the effect of different competitive ions on relative fluorescent signal change of $10 \mu\text{M}$ **FS** in DMSO:water (pH 8.0, 1:1 v/v) were insignificant when compared with response of Hg^{2+} ion that clearly showed selectivity of **FS** against to Hg^{2+} .

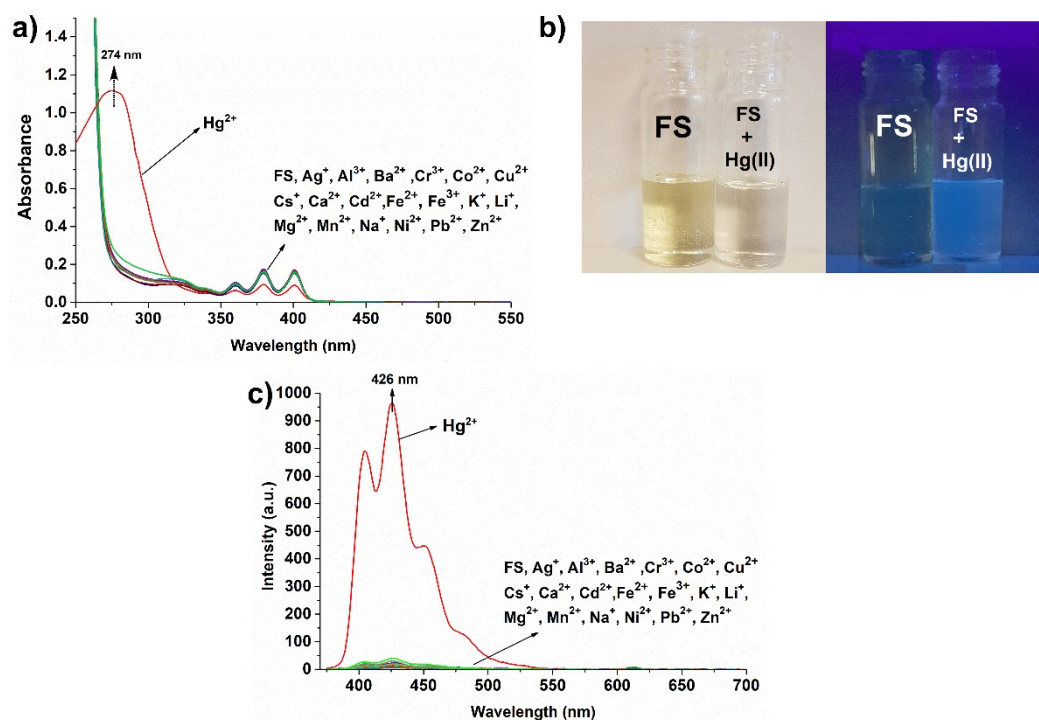


Figure 3: a) UV-vis electronic absorption, b) color change (daylight and 365 nm light source) and c) fluorescent emission spectra of $10 \mu\text{M}$ **FS** in DMSO:water (pH 8.0, 1:1 v/v) upon addition of $120 \mu\text{M}$ Hg^{2+} .

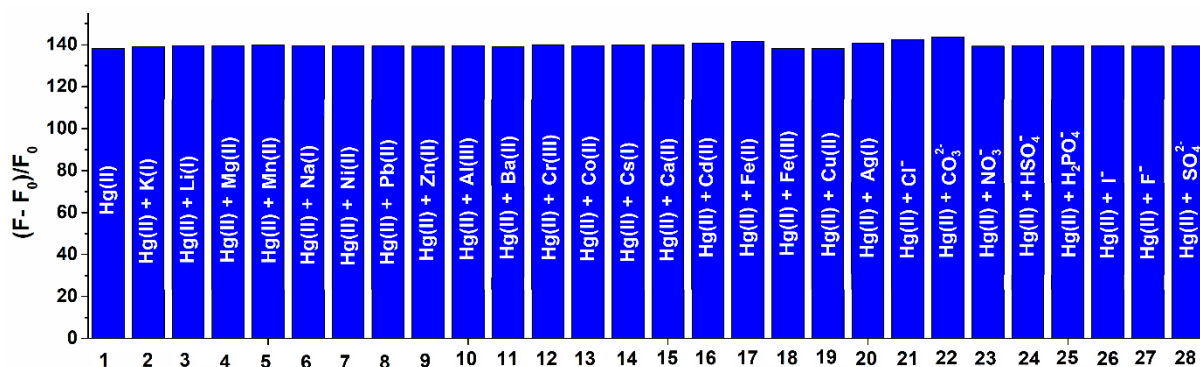


Figure 4: Relative fluorescent signal changes of 10 μM **FS** in DMSO:water (pH 8.0, 1:1 v/v, $\lambda_{\text{ex}}=360$ nm) upon addition of 120 μM Hg^{2+} + 2400 μM various metal ions.

The pH of analysis medium for fluorescent sensors which were designed for detection or determination of metal ions was important parameter, therefore, the effect of pH on relative fluorescent signal change of 10 μM **FS** in DMSO: water (1:1 v/v) with the addition of Hg^{2+} was investigated between pH 4 and 11 (29, 33) when other conditions kept steady. For that purpose, pH of 10 μM **FS** in DMSO: water (1:1 v/v) was adjusted by Britton-Robinson buffer (Figure 5a). As seen, the **FS**- Hg^{2+} complex is nearly pH-independent between pH 6.0–9.0 when considering the relative fluorescent signals. Therefore, the optimum pH was determined as 8.0 for the rest of the study, which demonstrated that **FS** could be used as a fluorescent sensor for spectrofluorimetric analysis of Hg^{2+} under neutral physical conditions (35). Then, the optimization of pH, effect of response time before the measurement was investigated for **FS** in DMSO: water (1:1 v/v) with the addition of Hg^{2+} ion when other parameters kept steady (Figure 5b). For that investigation, pH

of 10 μM **FS** DMSO:water (1:1 v/v) was adjusted 8.0 and 120 μM Hg^{2+} ion was added in this solution. Thereafter, obtained solution was carefully stirred up to 120 seconds and fluorescent spectra were recorded periodically. The results demonstrated that, after 60 seconds relative fluorescent signals remained nearly steady. Therefore, optimum time for measurement was determined as 60 second for determination of Hg^{2+} . To obtain accurate results in a spectrofluorimetric determination of a real sample using fluorescent sensors, the photostability of the sensor is highly essential. Accordingly, the photostability of **FS** and **FS**+ Hg^{2+} was investigated under optimized conditions. For that purpose, 120 μM of Hg^{2+} was added to 10 μM **FS** in DMSO:water (pH 8.0, 1:1 v/v) then stirred vigorously for 60 seconds and fluorescent responses observed between 1-60 minutes under daylight. As can be seen from Figure 5c, both **FS** and Hg^{2+} complex of **FS** was immensely photostable.

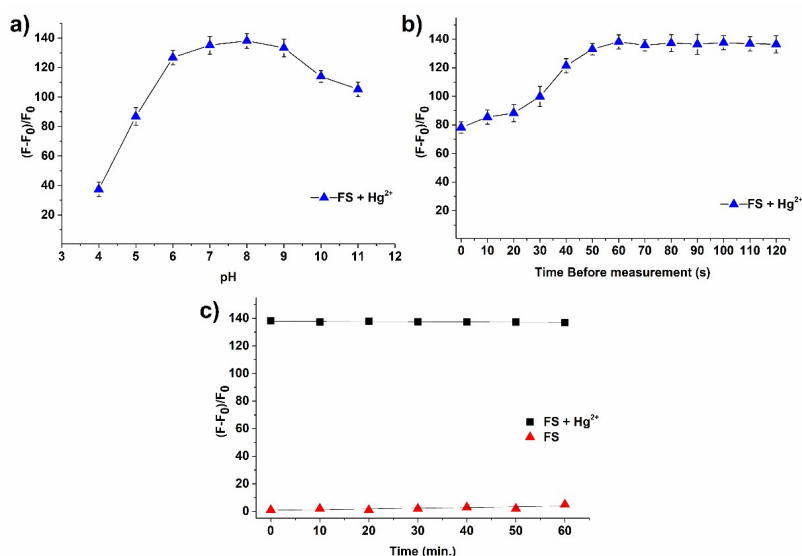


Figure 5: The effect of **a)** pH and **b)** measurement time on on relative fluorescent signal of **FS**+ Hg^{2+} and **c)** photostability of **FS** and **FS**+ Hg^{2+} (10 μM **FS** in DMSO:water (pH 8.0, 1:1 v/v, $\lambda_{\text{ex}}=360$ nm); 120 μM Hg^{2+}).

Complex formation of **FS** with Hg^{2+} ion was investigated by Job's plot (continuous variation) and non-linear curve fitting analysis in a buffered solution at pH 8.0 (36, 37). As can be seen from Figure 6a, maximum signal change was obtained at 0.5 in Job's plot, which revealed that stoichiometry of the **FS**- Hg^{2+} complex was 1:1. Besides, non-linear curve fitting analysis showed an inflection point at 1.0, which supports 1:1 binding mode (Figure 6b). With FT-IR analysis, we

obtained more information about the complexation of Hg^{2+} with **FS**, (Figure 6c). In the FT-IR spectrum of **FS**, -OH and C=N vibration peaks were observed at 3271 cm^{-1} and 1634 cm^{-1} , respectively. After treatment with Hg^{2+} , -OH vibration peak of **FS** disappeared, and the C=N vibration peak shifted to 1610 cm^{-1} proving that Hg^{2+} and **FS** had coordination via O- Hg^{2+} -N bond. According to the obtained results, the proposed binding mechanism for **FS**- Hg^{2+} was given in Figure 6d.

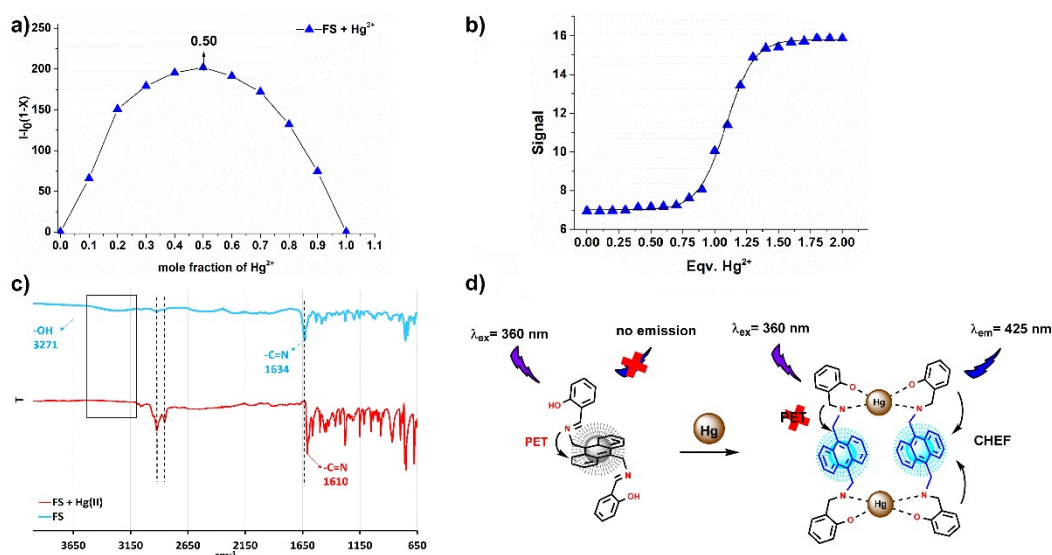


Figure 6: a) Job's Plot, b) non-linear curve fitting, c) FT-IR spectral analysis of **FS**+ Hg^{2+} and d) proposed binding mode for **FS**+ Hg^{2+} (10 μM **FS** in DMSO:water (pH 8.0, 1:1 v/v, λ_{ex} =360 nm).

Analytical Performance

The fluorescent response of **FS** towards to Hg^{2+} was also evaluated by fluorescent titration experiments under the optimized conditions (Figure 7a). As shown in Figure 7a, after gradual addition increased amount of Hg^{2+} to 10 μM **FS** in DMSO: water (pH 8.0, 1:1 v/v), fluorescent emission signal of **FS** at 426 nm was gradually and proportionally increased between 0.05-120.00 μM

Hg^{2+} which indicates the formation of **FS**+ Hg^{2+} complex. The calibration curve of **FS** for Hg^{2+} was given in Figure 7b, which demonstrated a good linear relationship ($R^2=0.9938$) between the relative fluorescent signal change and Hg^{2+} concentration between 0.05-120.00 μM . Also, linear regression equations for Hg^{2+} was determined as $(F-F_0)/F_0=1.1839[\text{Hg}^{2+}]-8.3709$.

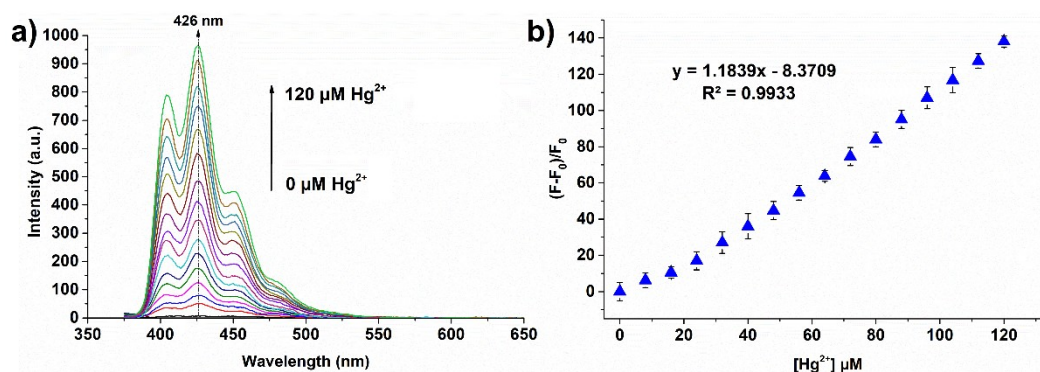


Figure 7: a) Fluorescent emission response of 10 μM **FS** in DMSO:water (pH 8.0, 1:1 v/v, λ_{ex} =360 nm) upon gradually addition of Hg^{2+} ion and b) calibration curve for Hg^{2+} ion.

The LOD, limit of detection, which calculated as dividing three times of the standard deviation of

the blank sample by the slope of the calibration graph ($3\sigma/K$) determined as 0.082 μM for Hg^{2+} ,

whereas the limit of quantification, LOQ, calculated as 0.246 μM for Hg^{2+} . Under optimized experimental conditions, the precision of the developed spectrofluorimetric determination method (N=10) was calculated as 2.58%, which assigned high precision and stability. All analytical parameters of **FS** for Hg^{2+} ion determination were given in Table 2. To evaluate the applicability of presented fluorescent sensor for

spectrofluorimetric analysis for Hg^{2+} in environmental water samples, **FS** was applied to seawater, lake, and tap water samples without any enhancement processes and obtained results given at Table 3. As seen in Table 3, obtained results for the spectrofluorimetric analysis of Hg^{2+} demonstrated high percentage recovery in environmental water samples and in a good agreement with to the spiked concentrations.

Table 2: Analytical parameters of **FS** for Hg^{2+} ion determination.

Excitation wavelength (nm)	360
Emission wavelength (nm)	426
Limit of detection (LOD) (μM)	0.082
Limit of quantification (LOQ) (μM)	0.245
Linear range (μM)	0.05-120
Optimum pH	8.0
Ligand concentration (μM)	2
Final volume (mL)	5
Solvent	DMSO:water (1:1 v/v)
Time before measurement (second)	60
Correlation coefficient (R ²)	0.9938
Precision (RSD%)	2.58

Table 3: Spectrofluorimetric determination of Hg^{2+} in environmental water samples using **FS**.

Water sample	Spiked concentration of Hg^{2+} ions (μM)	Found (μM)	Recovery (%)
Seawater	20.00	20.59±0.52	102.95
	40.00	40.32±0.96	100.80
Lake water	20.00	20.29±0.35	101.45
	40.00	39.52±0.84	98.80
Tap water	20.00	19.20±0.28	96.00
	40.00	38.92±1.01	97.30

CONCLUSION

In summary, simple, efficient, and accessible anthracene-based dipodal Schiff base "turn-on" fluorescent sensor for Hg^{2+} ion was designed and synthesized via high yield Schiff base reaction of salicylaldehyde and 9,10-bis(aminomethyl)anthracene. The characterization of **FS** was performed by MALDI-MS, FT-IR, ¹H and ¹³C NMR spectral methods. The photophysical and fluorescent sensor properties of **FS** were investigated by UV-Vis and fluorescent spectroscopies in different solvents. The presented fluorescent sensor demonstrated excellent selectivity and sensitivity towards Hg^{2+} over different competitive ions with "turn-on" response. The PET-triggered weak fluorescent response of **FS** was inhibited by coordination of Hg^{2+} via CHEF processes, and importantly "turn-on" fluorescent response was obtained at 426 nm. The binding mechanism of **FS** with Hg^{2+} was examined by electronic absorption and fluorescent spectroscopies. The LOD and LOQ were found to be 0.082 μM and 0.246 μM for Hg^{2+} , respectively. Finally, after the optimization of experimental conditions, spectrofluorimetric analysis of Hg^{2+} ions

was carried out in environmental water samples. According to obtained results, it can be said that **FS** is a selective and sensitive "turn-on" fluorescent sensor candidate for Hg^{2+} detection in aqueous media.

REFERENCES

- Duran C, Tumay SO, Ozdes D, Serencam H, Bektas H. Simultaneous separation and preconcentration of Ni(II) and Cu(II) ions by coprecipitation without any carrier element in some food and water samples. *International Journal of Food Science & Technology*. 2014;49(6):1586-92.
- Yan Z, Yuen M-F, Hu L, Sun P, Lee C-S. Advances for the colorimetric detection of Hg^{2+} in aqueous solution. *RSC Advances*. 2014;4(89):48373-88.
- Kim HN, Ren WX, Kim JS, Yoon J. Fluorescent and colorimetric sensors for detection of lead, cadmium, and mercury ions. *Chemical Society Reviews*. 2012;41(8):3210-44.

4. Taki M, Akaoka K, Iyoshi S, Yamamoto Y. Rosamine-Based Fluorescent Sensor with Femtomolar Affinity for the Reversible Detection of a Mercury Ion. *Inorganic Chemistry*. 2012;51(24):13075-7.
5. Liu D, Wang Y, Wang R, Wang B, Chang H, Chen J, et al. Fluorescein-based fluorescent sensor with high selectivity for mercury and its imaging in living cells. *Inorganic Chemistry Communications*. 2018;89:46-50.
6. Gao Y, De Galan S, De Brauwere A, Baeyens W, Leermakers M. Mercury speciation in hair by headspace injection-gas chromatography-atomic fluorescence spectrometry (methylmercury) and combustion-atomic absorption spectrometry (total Hg). *Talanta*. 2010;82(5):1919-23.
7. Tümay SO, Uslu A, Ardiç Alidağı H, Kazan HH, Bayraktar C, Yolaçan T, et al. A systematic series of fluorescence chemosensors with multiple binding sites for Hg(ii) based on pyrenyl-functionalized cyclotriphosphazenes and their application in live cell imaging. *New Journal of Chemistry*. 2018;42(17):14219-28.
8. Deng B, Xiao Y, Xu X, Zhu P, Liang S, Mo W. Cold vapor generation interface for mercury speciation coupling capillary electrophoresis with electrothermal quartz tube furnace atomic absorption spectrometry: Determination of mercury and methylmercury. *Talanta*. 2009;79(5):1265-9.
9. Mao Y, Liu G, Meichel G, Cai Y, Jiang G. Simultaneous Speciation of Monomethylmercury and Monoethylmercury by Aqueous Phenylation and Purge-and-Trap Preconcentration Followed by Atomic Spectrometry Detection. *Analytical Chemistry*. 2008;80(18):7163-8.
10. Nguyen TH, Boman J, Leermakers M, Baeyens W. Mercury analysis in environmental samples by EDXRF and CV-AAS. *Fresenius' Journal of Analytical Chemistry*. 1998;360(2):199-204.
11. Zheng C, Li Y, He Y, Ma Q, Hou X. Photo-induced chemical vapor generation with formic acid for ultrasensitive atomic fluorescence spectrometric determination of mercury: potential application to mercury speciation in water. *Journal of Analytical Atomic Spectrometry*. 2005;20(8):746-50.
12. Zhang C, Gao B, Zhang Q, Zhang G, Shuang S, Dong C. A simple Schiff base fluorescence probe for highly sensitive and selective detection of Hg²⁺ and Cu²⁺. *Talanta*. 2016;154:278-83.
13. Wei T-b, Gao G-y, Qu W-j, Shi B-b, Lin Q, Yao H, et al. Selective fluorescent sensor for mercury(II) ion based on an easy to prepare double naphthalene Schiff base. *Sensors and Actuators B: Chemical*. 2014;199:142-7.
14. Gujar V, Sangale V, Ottoor D. A Selective Turn off Fluorescence Sensor Based on Propranolol-SDS Assemblies for Fe³⁺ Detection. *Journal of Fluorescence*. 2019;29(1):91-100.
15. Kim K, Choi SH, Jeon J, Lee H, Huh JO, Yoo J, et al. Control of On-Off or Off-On Fluorescent and Optical [Cu²⁺] and [Hg²⁺] Responses via Formal Me/H Substitution in Fully Characterized Thienyl "Scorpionate"-like BODIPY Systems. *Inorganic Chemistry*. 2011;50(12):5351-60.
16. Long Y, Yang M-p, Yang B-q. Development and applications of two colorimetric and fluorescent indicators for Hg²⁺ detection. *Journal of Inorganic Biochemistry*. 2017;172:23-33.
17. Wang H, Li Y, Xu S, Li Y, Zhou C, Fei X, et al. Rhodamine-based highly sensitive colorimetric off-on fluorescent chemosensor for Hg²⁺ in aqueous solution and for live cell imaging. *Organic & Biomolecular Chemistry*. 2011;9(8):2850-5.
18. Burrell CN, Bodine MI, Elbjairami O, Reibenspies JH, Omary MA, Gabbai FP. Enhancement of External Spin-Orbit Coupling Effects Caused by Metal-Metal Cooperativity. *Inorganic Chemistry*. 2007;46(4):1388-95.
19. Coskun A, Akkaya EU. Signal Ratio Amplification via Modulation of Resonance Energy Transfer: Proof of Principle in an Emission Ratiometric Hg(II) Sensor. *Journal of the American Chemical Society*. 2006;128(45):14474-5.
20. Tian M, Ihmels H. Selective ratiometric detection of mercury(ii) ions in water with an acridinium-based fluorescent probe. *Chemical Communications*. 2009(22):3175-7.
21. Alizadeh K, Parooi R, Hashemi P, Rezaei B, Ganjali MR. A new Schiff's base ligand immobilized agarose membrane optical sensor for selective monitoring of mercury ion. *Journal of Hazardous Materials*. 2011;186(2):1794-800.
22. Quang DT, Wu J-S, Luyen ND, Duong T, Dan ND, Bao NC, et al. Rhodamine-derived Schiff base for the selective determination of mercuric ions in water media. *Spectrochimica Acta Part A: Molecular and Biomolecular Spectroscopy*. 2011;78(2):753-6.
23. Kaur B, Gupta A, Kaur N. A novel, anthracene-based naked eye probe for detecting Hg²⁺ ions in

aqueous as well as solid state media. *Microchemical Journal*. 2020;153:104508.

24. Zhou Y, Zhu C-Y, Gao X-S, You X-Y, Yao C. Hg²⁺-Selective Ratiometric and "Off-On" Chemosensor Based on the Azadiene-Pyrene Derivative. *Organic Letters*. 2010;12(11):2566-9.

25. Tümay SO, Yeşilot S. Tripodal synthetic receptors based on cyclotriphosphazene scaffold for highly selective and sensitive spectrofluorimetric determination of iron(III) in water samples. *Journal of Photochemistry and Photobiology A: Chemistry*. 2019;372:156-67.

26. Sie Y-W, Wan C-F, Wu A-T. A multifunctional Schiff base fluorescence sensor for Hg²⁺, Cu²⁺ and Co²⁺ ions. *RSC Advances*. 2017;7(5):2460-5.

27. Kaur B, Kaur N. Detection of Al³⁺ and Hg²⁺ ions with anthracene appended Schiff base and its reduced analogue. *Journal of Coordination Chemistry*. 2019;72(13):2189-99.

28. Ke C, Destecroix H, Crump MP, Davis AP. A simple and accessible synthetic lectin for glucose recognition and sensing. *Nature Chemistry*. 2012;4(9):718-23.

29. Mondal B, Banerjee S, Ray J, Jana S, Senapati S, Tripathy T. "Novel Dextrin-Cysteine Schiff Base: A Highly Efficient Sensor for Mercury Ions in Aqueous Environment". *ChemistrySelect*. 2020;5(6):2082-93.

30. Guven N, Camurlu P. Electrosyntheses of anthracene clicked poly(thienylpyrrole)s and investigation of their electrochromic

properties. *Polymer*. 2015;73:122-30.

31. Fery-Forgues S, Lavabre D. Are Fluorescence Quantum Yields So Tricky to Measure? A Demonstration Using Familiar Stationery Products. *Journal of Chemical Education*. 1999;76(9):1260.

32. Melhuish WH. QUANTUM EFFICIENCIES OF FLUORESCENCE OF ORGANIC SUBSTANCES: EFFECT OF SOLVENT AND CONCENTRATION OF THE FLUORESCENT SOLUTE¹. *The Journal of Physical Chemistry*. 1961;65(2):229-35.

33. Bayindir S. A simple rhodanine-based fluorescent sensor for mercury and copper: The recognition of Hg²⁺ in aqueous solution, and Hg²⁺/Cu²⁺ in organic solvent. *Journal of Photochemistry and Photobiology A: Chemistry*. 2019;372:235-44.

34. Xu Y, Mao S, Peng H, Wang F, Zhang H, Aderinto SO, et al. A fluorescent sensor for selective recognition of Al³⁺ based on naphthalimide Schiff-base in aqueous media. *Journal of Luminescence*. 2017;192:56-63.

35. Wee SS, Ng YH, Ng SM. Synthesis of fluorescent carbon dots via simple acid hydrolysis of bovine serum albumin and its potential as sensitive sensing probe for lead (II) ions. *Talanta*. 2013;116:71-6.

36. Chai SC, Lu J-P, Ye Q-Z. Determination of binding affinity of metal cofactor to the active site of methionine aminopeptidase based on quantitation of functional enzyme. *Anal Biochem*. 2009;395(2):263-4.

37. Chai SC, Ye Q-Z. Analysis of the stoichiometric metal activation of methionine aminopeptidase. *BMC Biochem*. 2009;10:32-.

